

Spontaneously Formed Vesicles of Sodium *N*-(11-Acrylamidoundecanoyl)-glycinate and L-Alaninate in Water

Sumita Roy and Joykrishna Dey*

Department of Chemistry, Indian Institute of Technology, Kharagpur 721 302, India

Received May 5, 2005. In Final Form: August 18, 2005

Two *N*-acyl amino acid surfactants, sodium *N*-(11-acrylamidoundecanoyl)-glycinate (SAUG) and L-alaninate (SAUA), were synthesized and characterized in aqueous solution. A number of techniques, such as surface tension, fluorescence probe, light scattering, and transmission electron microscopy were employed for characterization of the amphiphiles in water. The surface and interfacial properties were measured. The amphiphiles have two critical aggregation concentrations. The results of surface tension and fluorescence probe studies suggested formation of bilayer self-assemblies in dilute aqueous solutions of the amphiphiles. The magnitudes of free energy change of aggregation have indicated that bilayer formation is more favorable in the case of SAUG. Steady-state fluorescence measurements of pyrene and 1,6-diphenyl-1,3,5-hexatriene (DPH) were used to study the microenvironment of the molecular self-assemblies. Temperature-dependent fluorescence anisotropy change of DPH probe revealed phase transition temperature of the bilayer self-assemblies. The effects of pH on the structure of the self-assemblies of SAUG and SAUA have been studied. The role of intermolecular hydrogen bonding between amide groups upon aggregation toward microstructure formation in solution has been discussed. Circular dichroism spectra suggested the presence of chiral aggregates in an aqueous solution of SAUA. The transmission electron micrographs revealed the presence of closed spherical vesicles in aqueous solutions of the amphiphiles. Dynamic light scattering measurements were performed to obtain average size of the aggregates.

Introduction

Recently, *N*-acyl amino acid surfactants (NAAS) have attracted considerable attention mainly because of their chirality which is an important phenomenon in nature.¹ Further, the sodium salts of long-chain NAAS are currently used as detergents, foaming agents, and shampoos as they are mild, nonirritating to human skin, and easily biodegradable.² They have been also shown to be useful in stereoselective synthesis.³ The NAAS are a class of surfactants that show interesting aggregation properties in solution. The NAAS have been reported to self-organize in water^{1a,4} and also in organic solvents⁵ to form various

types of supramolecular structures. These supramolecular assemblies generate bilayers in water with shapes such as planar membranes, tubules, helices, ribbons, and rods. Among these, the tubules and helical ribbons are the most interesting as far as technological applications of nanostructured materials are concerned.⁶ It has been found that the chirality has a significant effect on the critical micelle concentration (cmc), on the formation of liquid crystals, and also on the melting point.^{7–9} For example, it has been shown that an optically active NAAS has a lower cmc than its racemic mixture.⁷ The optically active NAAS forms lyotropic liquid crystals different from the racemic mixture.⁸ Also it has been reported that assemblies formed from racemic mixtures have different morphologies¹⁰ from those formed by enantiomerically pure surfactant. One of the important effects of chirality is the enhanced lifetime of hydrophobic aggregates, which is commonly known as “chiral bilayer effect”. Indeed, vesicles formed by enantiomerically pure surfactant have been

* To whom correspondence should be addressed. Tel. 91-3222-283308. Fax. 91-3222-255303. E-mail: joydey@chem.iitkgp.ernet.in.

(1) (a) Du, X.; Hlady, V. *J. Phys. Chem. B* **2002**, *106*, 7295–7299. (b) Du, X.; Liang, Y. *J. Phys. Chem. B* **2001**, *105*, 6092–6096. (c) Du, X.; Liang, Y. *J. Phys. Chem. B* **2000**, *104*, 10047–10052. (d) Miyagishi, S.; Takeuchi, N.; Asakawa, T.; Inoh, M. *Colloid Surf. A: Physicochem. Eng. Aspects* **2002**, *197*, 125–132. (e) Bella, J.; Borocci, S.; Mancini, G. *Langmuir* **1999**, *15*, 8025–8031. (f) Borocci, S.; Mancini, G.; Cerichelli, G.; Luchetti, L. *Langmuir* **1999**, *15*, 2627–2630. (g) Hoffmann, F.; Huhnerfuss, H.; Stine, K. *J. Langmuir* **1998**, *14*, 4525–4534. (h) Parazak, D. P.; Uang, J. Y.-J.; Turner, B.; Stine, K. *J. Langmuir* **1994**, *10*, 3787–3793.

(2) (a) Takehara, M.; Moriyuki, H.; Yoshimura, I.; Yoshida, R. *J. Am. Chem. Soc.* **1972**, *49*, 143–150. (b) Takehara, M. *Colloids Surf.* **1989**, *38*, 149–167.

(3) (a) Zhang, Y.; Sun, P. *Tetrahedron: Asymmetry* **1996**, *7*, 3055–3058. (b) Takeshita, M.; Yanagihara, H.; Terada, K.; Akutsu, N. *Annu. Rep. Tohoku Coll. Pharm.* **1992**, *39*, 247. (c) Zhang, Y.; Wu, W. *Tetrahedron: Asymmetry* **1999**, *8*, 3575–3578. (d) Diego-Castro, M. J.; Hailes, H. C. *Chem. Commun.* **1998**, 1549–1550.

(4) (a) Zhang, Y.-J.; Jin, M.; Lu, R.; Song, Y.; Jiang, L.; Zhao, Y.; Li, T. *J. Phys. Chem. B* **2002**, *106*, 1960–1967. (b) Boettcher, C.; Schade, B.; Fuhrhop, J.-H. *Langmuir* **2001**, *17*, 873–877. (c) Imae, T.; Takahashi, Y.; Muramatsu, H. *J. Am. Chem. Soc.* **1992**, *114*, 3414–3419. (d) Vollhardt, D.; Gehlert, U. *J. Phys. Chem. B* **2002**, *106*, 4419–4423. (e) Kawasaki, H.; Souda, M.; Tanaka, S.; Nemoto, N.; Karlsson, G.; Almgren, M.; Maeda, H. *J. Phys. Chem. B* **2002**, *106*, 1524–1527. (f) Fuhrhop, J.-H.; Demoulin, C.; Rosenberg, J.; Boettcher, C. *J. Am. Chem. Soc.* **1990**, *112*, 2827–2829.

(5) (a) Shinitzky, M.; Haimovitz, R. *J. Am. Chem. Soc.* **1993**, *115*, 12545–12549. (b) Song, J.; Cheng, Q.; Kopta, S.; Stevens, R. C. *J. Am. Chem. Soc.* **2001**, *123*, 3205–3213. (c) Bhattacharyya, S.; Krishnan-Ghosh, Y. *Chem. Commun.* **2001**, 185–186. (d) Luo, X.; Liu, B.; Liang, Y. *Chem. Commun.* **2001**, 1556–1557.

(6) (a) Yager, P.; Schoen, P. *Mol. Cryst. Liq. Cryst.* **1984**, *106*, 371–381. (b) Schnur, J. M. *Science* **1993**, *262*, 1669–1676.

(7) (a) Miyagishi, S.; Nishida, M. *J. Colloid Interface Sci.* **1978**, *65*, 380–386. (b) Miyagishi, S.; Higashide, M.; Asakawa, T.; Nishida, M. *Langmuir* **1991**, *7*, 51–55. (c) Takehara, M.; Yoshimura, I.; Yoshida, R. *J. Am. Chem. Soc.* **1974**, *51*, 419–423.

(8) (a) Tracey, A. S.; Radley, K. *Langmuir* **1990**, *6*, 1221–1224. (b) Tracey, A. S.; Radley, K. *Mol. Cryst. Liq. Cryst.* **1985**, *122*, 77–87. (c) Tracey, A. S.; Radley, K. *J. Phys. Chem.* **1984**, *88*, 6044–6048. (d) Radley, K.; Tracey, A. S. *Can. J. Chem.* **1985**, *63*, 95–99.

(9) (a) Miyagishi, S.; Matsumura, S.; Murata, K.; Asakawa, T.; Nishida, M. *Bull. Chem. Soc. Jpn.* **1985**, *58*, 1019–1022. (b) Miyagishi, S.; Matsumura, S.; Murata, K.; Asakawa, T.; Nishida, M. *Bull. Chem. Soc. Jpn.* **1986**, *59*, 557–561.

(10) Fuhrhop, J.-H.; Schnieder, P.; Rosenberg, J.; Boekema, E. *J. Am. Chem. Soc.* **1987**, *109*, 3387–3390.

shown to be more stable compared to racemic ones under the same condition.¹¹ It has been shown that the nature of vesicular structures used for controlled drug delivery depends on the stereochemistry of the chiral amphiphile.¹² It has been found that change in the headgroup and the hydrocarbon tail affects the morphology. In fact, the hydrophobic interaction between long hydrocarbon chains is essential in the formation of supramolecular aggregates, and the interaction between headgroups is a possible driving force for the formation of helical and/or cylindrical aggregates.

In this work, we have synthesized two new NAAS, sodium *N*-(11-acrylamidoundecanoyl)-glycinate (SAUG) and *L*-alaninate (SAUA) (see Figure 4 for structures) the hydrophilic headgroup of which is a simple α -amino acid. The long hydrophobic tail of the NAAS has an amide group at the end, which may facilitate hydrogen bond formation and hence inhibit the chain mobility. Indeed, in a recent paper, we have demonstrated that hydrogen bonding interactions between hydrophobic tails of sodium *N*-11-acrylamidoundecanoate (SAU) result in the formation of bilayer aggregates in aqueous solution.¹³ The hydrophobic tail having length equal to that of a C_{16} chain is suitable for the formation of stable vesicles. The focus of the present work are (i) to investigate the aggregation behavior of SAUA, and SAUG in aqueous solution, (ii) to study the microenvironment of the self-assemblies, (iii) to determine the mean size of the self-assemblies, (iv) to examine the effect of chirality of the surfactant headgroup, and (v) to investigate the microstructures of the self-assemblies in solution. The circular dichroism (CD) spectra of SAUA were measured to examine formation of chiral self-assemblies.

Experimental Section

Materials. The fluorescence probes pyrene, 1-anilino-naphthalene, and 1,6-diphenyl-1,3,5-hexatriene (Aldrich) were recrystallized from acetone-ethanol mixture at least three times. Purity of the compounds was tested by the fluorescence emission and excitation spectra. Acryloyl chloride (Aldrich) and 11-amino-undecanoic acid (Aldrich), *N*-hydroxysuccinimide (SRL), dicyclohexylcarbodiimide (SRL), glycine, and *L*-alanine (SRL) were used without further purification. Analytical grade sodium hydroxide, sodium bicarbonate, sodium dihydrogen phosphate, disodium hydrogen phosphate, sodium acetate, sodium chloride, and hydrochloric acid were procured locally and were used directly from the bottle. All solvents used were of good quality commercially available and whenever necessary purified, dried and distilled fresh before use.

Synthesis. *N*-(11-acrylamidoundecanoyl)-*L*-alanine (AUA) was synthesized from *N*-hydroxysuccinimide ester of *N*-11-acrylamidoundecanoic acid (AUA) and *L*-alanine by slight modification of the method reported in the literature.¹⁴ The AUA was synthesized and purified according to the procedure described elsewhere.¹⁵ The optical activity was established by measurement of specific rotation of the acid. The other amphiphile, SAUG in its acid form, was also synthesized by the same method. The molecular structures of the compounds were determined by elemental analysis, ¹H NMR, and IR spectra. The details of chemical identifications of the molecules have been included in the Supporting Information.

The sodium salts were prepared by stirring the respective acid in water-tetrahydrofuran mixture containing equimolar

sodium bicarbonate for 18 h. The salt was obtained as solid mass after evaporation of the solvent. The crude salt was recrystallized from petroleum ether-ethanol mixture several times.

Methods. General Instrumentation. ¹H NMR spectra were recorded on a Bruker SEM 200 instrument in CDCl₃ solvent using TMS as standard. The UV-visible spectra were recorded in a Shimadzu (model 1601) spectrophotometer. The optical rotation was measured with a Jasco P-1020 digital polarimeter. The CD spectra were recorded on a Jasco, J-810 spectropolarimeter using quartz cells of 2 or 10 mm path length. Melting points were determined with a Instind (Kolkata) melting point apparatus in open capillaries. The pH measurements were done with a digital pH meter Model pH 5652 (EC India Ltd., Calcutta) using a glass electrode. Conductivity measurements were performed with a Thermo Orion conductivity meter (model 150 A+) by use of a cell having cell constant equal to 0.467 cm⁻¹. All measurements were carried out at room temperature (~30 °C) unless otherwise mentioned.

Surface Tension. The surface tension (γ) measurements were performed with a Torsion Balance (Hurdson & Co., Kolkata) using Du Nuoy ring detachment method. The platinum-iridium ring was regularly cleaned with ethanol-HCl solution. Stock solutions of the surfactants were made in Milli-Q water (18.2 M Ω). Aliquot of this solution was transferred to a beaker containing known volume of water. The solution was gently stirred magnetically and allowed to stand for about 5 min at room temperature (~30 °C) and then surface tension was measured. For each measurement, at least three readings were taken and the mean γ value was recorded. Before each experiment the instrument was calibrated and checked by measuring the surface tension of distilled water.

Steady-State Fluorescence. The steady-state fluorescence spectra were measured on a SPEX Fluorolog-3 spectrophotometer. Saturated solutions of pyrene and 1-anilino-naphthalene (AN) were made in Milli-Q water. The solutions containing pyrene and AN probe were excited at 335 and 340 nm, respectively. The emission spectrum was measured in the wavelength range of 350 to 550 nm. Each spectrum was blank subtracted and was corrected for lamp intensity variation during measurement. The excitation and emission slit widths were both set at 1 nm. Each measurement was repeated at least three times and the mean value was recorded.

Steady-state fluorescence anisotropy (r) was measured on a Perkin-Elmer LS-55 luminescence spectrometer equipped with filter polarizers that uses the L-format configuration. The temperature of the water-jacketed cell holder was controlled by use of a Thermo Neslab (RTE 7) circulating bath. Since DPH is insoluble in water, a 2 mM stock solution of the probe in 20% (v/v) methanol-water mixture was prepared. The final concentration of the probe was adjusted to 2 μ M by addition of an appropriate amount of the stock solution. The sample was excited at 350 nm and the emission intensity was followed at 450 nm using excitation and emission slits with band-pass of 2.5 and 5 nm, respectively. A 390 nm cutoff filter was placed in the emission beam to eliminate scattered radiation. The r value was calculated employing the equation

$$r = (I_{VV} - GI_{VH}) / (I_{VV} + 2GI_{VH}) \quad (1)$$

where I_{VV} and I_{VH} are the fluorescence intensities polarized parallel and perpendicular to the excitation light, and G is the instrumental correction factor ($G = I_{VV}/I_{VH}$).

Dynamic Light Scattering (DLS). The DLS measurements were performed with a Photal DLS-7000 (Otsuka Electronics CO. Ltd., Osaka, Japan) optical system equipped with an Ar⁺ ion laser (75 mW) operated at 16 mW at $\lambda = 488$ nm, a digital correlator, and a computer-controlled and stepping-motor-driven variable angle detection system. A 5.0 mM solution of the amphiphile was prepared in Milli-Q water. The solution was filtered directly into the scattering cell through a Millipore Millex syringe filter (Triton free, 0.22 μ m). Before measurement, the scattering cell was rinsed several times with the filtered solution. The DLS measurements started 5–10 min after the sample solutions were placed in the DLS optical system to allow the sample to equilibrate at the bath temperature. For all light scattering measurements, the temperature was 25 ± 0.5 °C. The scattering intensity was at angles

(11) Morigaki, K.; Dallavalle, S.; Walde, P.; Colonna, S.; Luisi, P. L. *J. Am. Chem. Soc.* **1997**, *119*, 292–301.

(12) Fuhrhop, J.-H.; Helfrich, W. *Chem. Rev.* **1993**, 1565–1582. (b) Jaeger, D.; Kubicz-Loring, E.; Price, R. C.; Nakagawa, H. *Langmuir* **1996**, *12*, 5803–5808.

(13) Roy, S.; Dey, J. *Langmuir* **2003**, *19*, 9625–9629.

(14) Lapidot, Y.; Rappoport, S.; Wolman, Y. *J. Lipid Res.* **1967**, *8*, 142–145.

(15) Yeoh, K. W.; Chew, C. H.; Gan, L. M.; Koh, L. L.; Teo, H. H. *J. Macromol. Sci. Chem. A* **1989**, *26*, 663–680.

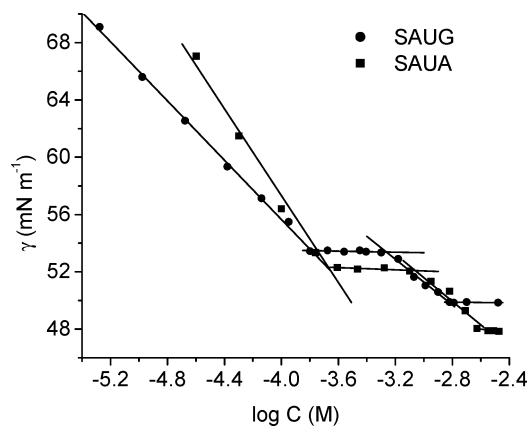


Figure 1. γ - $\log C$ plots of SAUG and SAUA in water (pH = 8.0).

in the range 45° – 135° to the incident beam. The data acquisition was carried out for 10 min and each experiment was repeated two or three times. The data were analyzed by cumulant method using the software provided by the manufacturer.

Transmission Electron Microscopy (TEM). The microscopic measurements were performed using a 5 mM solution of the amphiphiles. The surfactant solution was filtered by use of Millipore Millex syringe filter (Triton free, $0.22 \mu\text{m}$). A carbon-coated copper grid was dipped in a drop of the aqueous solution of the amphiphile, blotted with filter paper, and negatively stained with a freshly prepared 1% aqueous uranyl acetate or 2% phosphotungstate solution. The specimens were examined on a Phillips CM 200 electron microscope operating at 200 kV at room temperature ($\sim 25^\circ\text{C}$).

Results and Discussion

Surface Tension Studies. The surface tension method is the most versatile among all the methods that are used to estimate critical aggregation concentration (cac). This is not only because the cac can be obtained from the plots of surface tension (γ) versus $\log(\text{concentration})$ but also one can extract information on the nature of adsorbed layers at the air/water interface. The plots of γ vs $\log C$ for the aqueous solutions (pH = 8) of the amphiphiles are shown in Figure 1. The cac values of the amphiphiles were determined from the break points of the respective plot. It is interesting to see that there are two break points in both plots. The first break gives the cac of the surfactant. The second break may be due to the onset of secondary aggregation of the surfactant. Such types of post micellar aggregation have also been reported in the literature.^{16–18} In fact, three transition points (the cmc, micellar growth, and micellar entanglement) observed for many anionic surfactant have been reported in the literature.^{19,20} It should be noted here that the sodium salt of the precursor acid, SAU, has only one cac (0.4 mM).¹³ Therefore, the

Table 1. Critical Aggregation Concentrations (cac), Critical Vesicle Concentration (cvc), Surface Tension (γ_{cac}) and Surface Pressure (π_{cac}) at cac, Surface Excess Concentration (Γ_2), Surface Area Per Molecule (a_0), Degree of Counterion Dissociation (α), and Standard Free Energy Change of Aggregation (ΔG_a°) and Adsorption ($\Delta G_{\text{ad}}^\circ$) of SAUG and SAUA in Aqueous Solutions (pH = 8.0) at 303 K

properties	SAUG	SAUA
cac (mM)	0.15, 0.11 ^a	0.22, 0.23 ^a
cvc (mM)	1.50, 1.82 ^a	2.54, 2.38 ^a
γ_{cac} (mN m ⁻¹)	53.5	52.3
π_{cac} (mN m ⁻¹)	17.7	18.9
$\Gamma_2 \times 10^6$ (mol m ⁻²)	1.66	1.60
a_0 (nm ²)	1.00	1.04
α	0.93	0.93
ΔG_a° (kJ mol ⁻¹)	-23.7	-22.7
$\Delta G_{\text{ad}}^\circ$ (kJ mol ⁻¹)	-34.4	-34.5

^a Data obtained from fluorescence measurement.

post micellar aggregation must be caused by the amide linkage near the surfactant headgroup. The cac and γ_{cac} values of the amphiphiles are listed in Table 1. The γ_{cac} values indicate that the amphiphiles are reasonably good surface-active agents. The γ_{cac} value of SAUA is slightly lower than that of SAUG. It can also be observed that both cac values of SAUG are less than the corresponding value of SAUA. This is consistent with the relatively bulky amino acid headgroup of the latter surfactant. Miyagishi and co-workers, however, have reported an opposite trend in γ_{cmc} and cmc values for sodium *N*-dodecanoylglycinate and *N*-dodecanoylalaninate surfactants.²¹ These authors have shown that with the increase in size of the amino acid side chain of the surfactant headgroup both cmc and γ_{cmc} value decreases.

Interfacial Properties. The surface tension measurements also allow one to determine the surface area per surfactant molecule at the interface which can be calculated from the slope of the linear part using the Gibb's adsorption equation^{17a}

$$\Gamma_2 = -1/(2.303nRT) (d\gamma/d\log C) \quad (2)$$

$$a_0 = 10^{18}/(\Gamma_2 N_A) \quad (3)$$

where Γ_2 is the maximum surface excess concentration expressed in mol m⁻², a_0 is the minimum surface area (in nm²) per surfactant molecule at the air/water interface, γ is surface tension in mN m⁻¹, N_A is the Avogadro number, $R = 8.314 \text{ J mol}^{-1} \text{ K}^{-1}$, and $n = 2$ for dilute solutions of monovalent ionic surfactants.²² The Γ_2 and a_0 values of the surfactants thus obtained are listed in Table 1. For both surfactants, the a_0 value is in the range $1.0 \text{ nm}^2 \leq a_0 \leq 1.1 \text{ nm}^2$, which is indicative of formation of bilayer aggregates.^{18a}

The standard free energy of adsorption ($\Delta G_{\text{ad}}^\circ$) of the surfactant at the air–water interface can be evaluated by use of the equation²³

$$\Delta G_{\text{ad}}^\circ = \Delta G_a^\circ - \pi_{\text{cac}} \Gamma_2 \quad (4)$$

where π_{cac} is the surface pressure ($= \gamma_0 - \gamma_{\text{cac}}$, γ_0 is the surface tension of pure water), and ΔG_a° is the standard free energy change of aggregation per mole of surfactant

(16) (a) Ptak, M.; Egret-Charlier, M.; Sanson, A.; Bouloussa, O. *Biochim. Biophys. Acta* **1980**, *600*, 387–397. (b) Tanford, C.; Nozakki, Y.; Rohde, M. F. *J. Phys. Chem.* **1977**, *81*, 1555–1560.

(17) (a) Chu, B.; Zhou, Z. *Physical Chemistry of Polyalkylene Block Copolymer Surfactants*. In *Nonionic Surfactants*; Nace, V. M., Ed.; Surfactant Science Series; M. Dekker: New York, 1996; Vol. 60, p 67. (b) Bhattacharya, S.; Haldar, J. *Langmuir* **2004**, *20*, 7940–7947.

(18) (a) Won, Y.-Y.; Brannan, A. K.; Davis, H. T.; Bates, F. S. *J. Phys. Chem. B* **2002**, *106*, 3354–3364. (b) Ghosh, H. N.; Palit, D. K.; Sapre, A. V.; Ramarao, K. V. S.; Mittal, J. P. *Chem. Phys. Lett.* **1993**, *203*, 5–11.

(19) Miyagishi, S.; Kurimoto, H.; Asakawa, T. *Langmuir* **1995**, *11*, 2951–2956.

(20) (a) Miyagishi, S.; Kurimoto, H.; Asakawa, T. *Bull. Chem. Soc. Jpn.* **1995**, *68*, 135–139. (b) Miyagishi, S.; Suzuki, H.; Asakawa, T. *Langmuir* **1996**, *12*, 2900–2905. (c) Miyagishi, S.; Akasofu, W.; Hashimoto, T.; Asakawa, T. *J. Colloid Interface Sci.* **1996**, *184*, 527–534.

(21) Miyagishi, S.; Asakawa, T.; Nishida, M. *J. Colloid Interface Sci.* **1989**, *131*, 68–73.

(22) Rosen, M. J. *Surfactants and Interfacial Phenomena*, 3rd ed.; Wiley-Interscience: New York, 2004; pp 60–64.

(23) Mukherjee, P. *Adv. Colloid Interface Sci.* **1967**, *1*, 242–275.

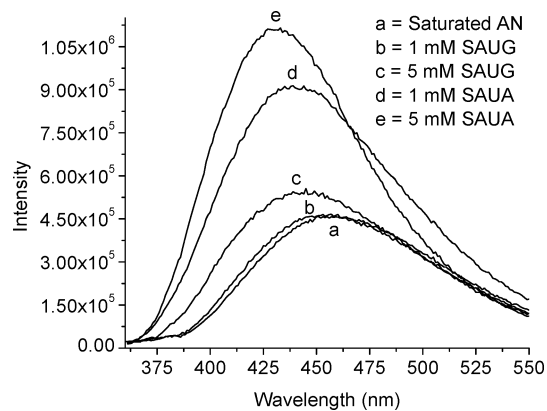


Figure 2. Fluorescence spectra of AN probe in water (pH = 8.0) in the presence of SAUG and SAUA.

molecule. ΔG_a° can be obtained by use of the equation²⁴

$$\Delta G_a^\circ = (2 - \alpha)RT \ln(cac/C_r) \quad (5)$$

where α is the degree of counterion dissociation and C_r ($= 1 \text{ mol L}^{-1}$) is the reference concentration. The α value (0.93) was determined by conductivity measurement the details of which are available in the Supporting Information. The ΔG_a° and ΔG_{ad}° values thus determined are tabulated in Table 1. It can be found that the ΔG_a° for SAUG is slightly more negative in comparison to that of SAUA. That is the aggregation is more favorable in the case of SAUG. This is consistent with the lower cac of SAUG compared to that of SAUA.

Fluorescence Probe Studies of the Self-Assemblies. Three different fluorescent molecules, AN, pyrene, and DPH, were used as extrinsic probes for the hydrophobic regions in the self-assemblies of SAUG and SAUA. These probe molecules bind preferentially to the hydrophobic domains resulting in enhancement of fluorescence intensity, shift of the emission maximum (λ_{max}) or change in fluorescence anisotropy. Therefore, the fluorescence characteristics of these probes when bound to the hydrophobic domains can shed light on aggregate structure.

The AN probe is weakly fluorescent in water. However, its fluorescence intensity increases manifold when dissolved in nonpolar solvents accompanied by a large blue shift of the emission maximum. Since it is hydrophobic and poorly soluble in water, it has been used as a probe molecule to study the change of microenvironment of its solubilization site. The fluorescence spectra of AN in the presence of two different concentrations (below and above the second cac) of SAUG and SAUA are shown in Figure 2. In presence of SAUA, the emission λ_{max} shifted toward shorter wavelengths within a relatively narrow concentration range around the cac indicating solubilization of AN within hydrophobic domains. Upon further increase of surfactant concentration, a small blue-shift accompanied by an increase of intensity was observed for SAUA. On the other hand, in the case of SAUG, neither emission λ_{max} nor intensity of AN shows any significant change around the first transition. At higher concentrations, a small blue shift of emission λ_{max} accompanied by a small increase of intensity can be observed. That is, the fluorescence intensity as well as emission λ_{max} of AN undergoes a distinct two-step change (not shown) with the increase of surfactant concentration. This is consistent

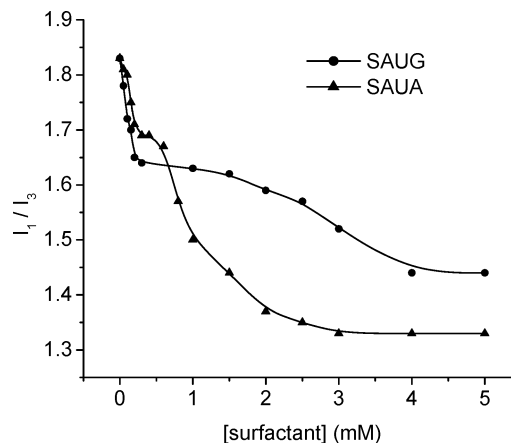


Figure 3. Plot of polarity ratio I_1/I_3 versus surfactant concentration of aqueous (pH = 8.0) SAUG and SAUA.

with the surface tension plot in Figure 1. The small blue shift of the emission λ_{max} and intensity change of AN fluorescence around the cac suggest formation of either small premicellar aggregates or large nonspherical aggregates in which the probe molecule is solvent exposed. The possibility of formation of premicellar aggregates can be ruled out, as such structure formation does not normally exhibit a break in the surface tension plot. The results also suggest that the microenvironment around the probe molecule is more hydrophobic in the case of SAUA. This is perhaps due to the bulky amino acid headgroup in SAUA, which reduces charge repulsion and thereby increases packing of the hydrocarbon tails of the surfactant molecules in the aggregate.

The hydrophobicity of the microenvironment of the self-assemblies was also measured by use of pyrene as fluorescence probe. The intensity ratio, I_1/I_3 , of the first and the third vibronic peaks of the pyrene fluorescence spectrum is known to be sensitive to polarity of its environment.²⁵ The I_1/I_3 ratio which has the highest value in water decreases with the decrease in solvent polarity. Therefore, it has been widely used as a micropolarity probe for self-assemblies.^{26,27} The polarity ratio was measured in the presence of different concentrations of SAUG and SAUA. The representative plots of I_1/I_3 versus surfactant concentration are shown in Figure 3. A two-step change is clearly evident from the plots. This is also consistent with the surface tension studies. The cac values (Table 1) obtained from the inflection points of the plots in Figure 3 are close to the corresponding values determined by surface tension measurements. The I_1/I_3 ratios (Table 2) for both surfactants are less compared to that in water (1.81), which indicates that the pyrene molecule is solubilized in hydrophobic environment of the self-assemblies.²⁶ Within the margin of experimental error the I_1/I_3 ratios just above the first break are equal. Since the polarity ratio corresponding to first state is high, the probe molecule is partially exposed to the bulk solvent. This as discussed earlier suggests that the probe molecules are solubilized within nonspherical aggregates such as bilayer structures as indicated by the a_0 values. The hydrocarbon layers of flat bilayer structures are expected to be exposed more to bulk solvent. However, hydrocarbon chains of spherical aggregates have less contact with water

(24) Moulik, S. P.; Haque, M. E.; Jana, P. K.; Das, A. R. *J. Phys. Chem.* **1996**, *100*, 701–708.

(25) Kalyanasundaram, K.; Thomas, J. K. *J. Am. Chem. Soc.* **1977**, *99*, 2039–2044.

(26) Zana, R. In *Surfactant Solutions. New Methods of Investigation*; Zana, R., Ed.; M. Dekker: New York, 1987; Chapter 5.

(27) Dong, D. C.; Winnik, M. A. *Photochem. Photobiol.* **1982**, *35*, 17.

Table 2. Micropolarity (I_1/I_3), pK_a , Phase Transition Temperature (T_m), Diffusion Constant (D), Hydrodynamic Radius (R_h), Mean Aggregation Number (N_{agg}) of SAUG and SAUA Vesicles in Water (pH 8.0)^a

properties	SAUG	SAUA
I_1/I_3	1.63 (1.42)	1.67 (1.30)
pK_a	6.20	6.70
T_m (K)	315	313
$D \times 10^{12}$ (m ² s ⁻¹)	4.15	6.24
R_h (nm)	62.0	42.0
$N_{agg} \times 10^{-4}$	10.5	4.26

^a Values in the brackets represent corresponding quantities above the cvc.

molecules. Consequently, pyrene molecules, which are normally, solubilized in the hydrocarbon layer encounter very few or no water molecules around them in the case of spherical aggregates. This is reflected by the low value of polarity ratio. The lower micropolarity of the secondary aggregates compared to that of primary aggregates suggests more ordering at the interface and perhaps formation of spherical vesicles at concentrations above the second break. The ordering of the aggregate interface reduces the degree of water penetration in the hydrocarbon layer, in accordance with the reduction observed in micropolarity sensed by the probe molecules. It is interesting to note that the microenvironment of the probe in SAUA vesicles is slightly more hydrophobic as compared to that in SAUG vesicles. This as discussed above is due to the bulky amino acid headgroup of SAUA.

To further understand the structural change that occurs at concentrations above the cac of the amphiphiles, we performed steady-state fluorescence anisotropy (r) measurements. The value of r can provide useful insights into the physical properties of lipid bilayers. The r is an index of equivalent microviscosity (more appropriately microfluidity) in the vesicle lipidic core. The DPH is a well-known membrane fluidity probe and has been used for studying many lipid bilayer membranes.²⁸ Fluorescence anisotropy of DPH was therefore measured at various concentrations above the cac for both surfactant solutions at room temperature. The anisotropy is relatively high at concentrations just above the first transition, which remained unchanged with the increase of surfactant concentration. The relatively high value of r suggests an ordered environment around the DPH probe in the self-assemblies. This may be due to hydrogen-bonding interactions among the amide groups of two neighboring surfactant molecules in the aggregate as shown in Figure 4. The r values in 5 mM SAUG (0.22) and SAUA (0.18) solutions were found to be greater than that of lecithin liposomes ($r \sim 0.098$) but less than that of sphingomyelin liposomes ($r \sim 0.247$).²⁹ Thus, it can be concluded that the nonspherical aggregates that are formed above the cac have flat bilayer structures. The large value of r and the decrease of micropolarity with the increase of surfactant concentration suggest that the flat bilayer aggregates are transformed into closed vesicles. Therefore, the concentration corresponding to the second break in the surface tension plot (Figure 1) can be taken as the critical vesicle concentration (cvc). The vesicle formation has been further confirmed by the conductivity study described below.

(28) (a) Shinitzky, M.; Dianoux, A.-C.; Itler, C.; Weber, G. *Biochemistry* **1971**, *10*, 2106–2113. (b) Shinitzky, M.; Yuli, I. *Chem. Phys. Lipids* **1982**, *30*, 261–282. (c) Shinitzky, M. In *Physical Methods on Biological Membranes and their Model Systems*; Plenum Publishing Corp.: New York, 1984; p 237.

(29) Shinitzky, M.; Barenholz, Y. *J. Biol. Chem.* **1974**, *249*, 2652–2657.

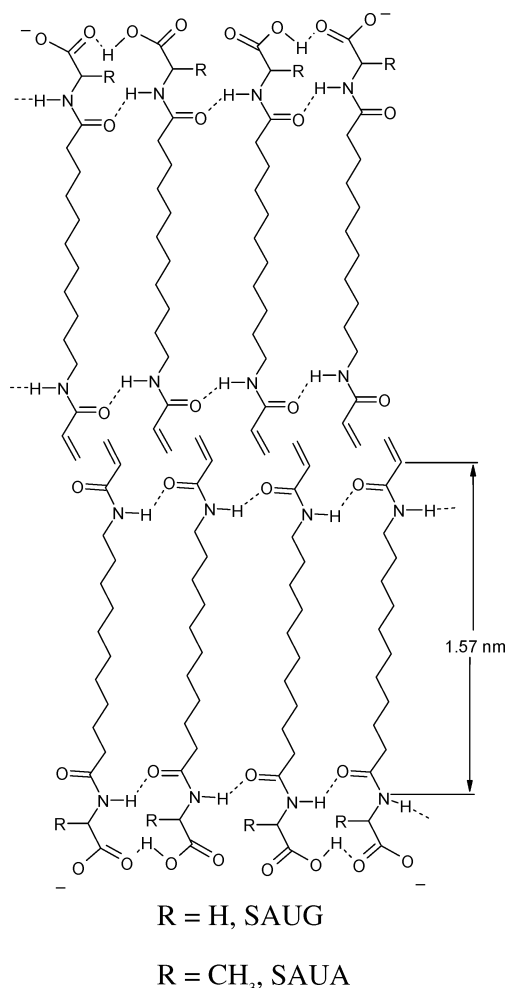


Figure 4. Schematic presentation of the bilayer structure of surfactant.

Conductivity Measurements. Hoffmann and co-workers³⁰ have reported a decrease of conductivity of KCl solution due to formation of vesicles by cetyltrimethylammonium 3-hydroxy-naphthalene-2-carboxylate surfactant in water. To demonstrate the transformation of the lamellar structure to closed vesicles, we have measured the conductivity of a 1 mM KCl solution in the presence of surfactant at 30 °C. It was found that the sum of the conductivities of 1 mM KCl (130.5 $\mu\text{S cm}^{-1}$) and 5 mM SAUG surfactant (421.4 $\mu\text{S cm}^{-1}$) solutions was greater than that of 1 mM KCl containing 5 mM surfactant solution (540 $\mu\text{S cm}^{-1}$). This means that the conductivity of the KCl solution decreased by $\sim 12.0 \mu\text{S cm}^{-1}$ in the presence of 5 mM (>cvc) SAUG. Similar decrease of conductivity ($\sim 10.0 \mu\text{S cm}^{-1}$) was also observed in the case of the SAUA surfactant. On the other hand, in the presence of 0.5 mM (<cvc) surfactant no significant decrease of conductivity of the KCl solution was observed. The variations of conductivity change ($\Delta\kappa$) with the increase of surfactant concentration for both surfactants are shown in Figure 5. It can be observed that $\Delta\kappa$ initially increases with surfactant concentration and then fall off passing through a maximum. This is a clear evidence of the formation of vesicles. The vesicles entrap a part of the solvent and the salt and consequently prevent the entrapped charge carriers (K^+ and Cl^- ions) from contributing to the conductivity of the solution. Consequently,

(30) Horbaschek, K.; Hoffmann, H.; Thunig, C. *J. Colloid Interface Sci.* **1998**, *206*, 439–456.

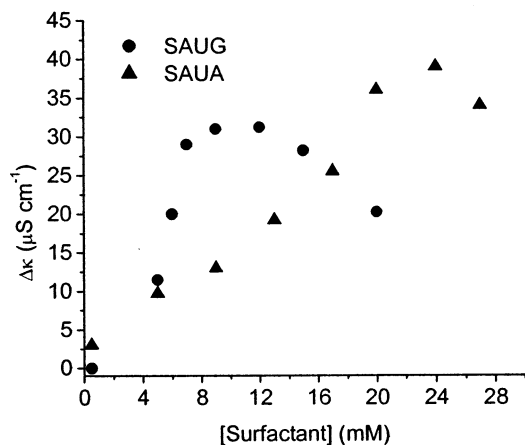


Figure 5. Plot of $\Delta\kappa$ versus surfactant concentration in water (pH = 8.0).

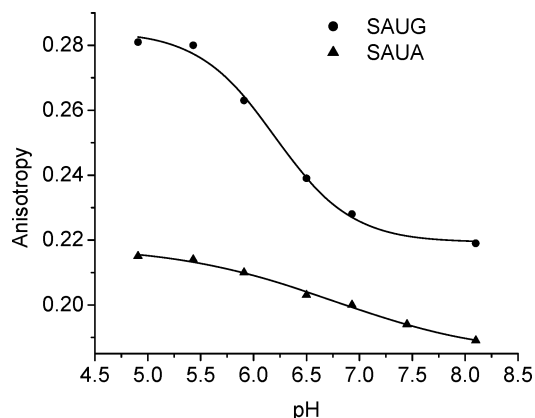


Figure 6. Plot of fluorescence anisotropy of DPH in the presence of 1 mM SAUG and SAUA as a function of pH.

the conductivity of the vesicular solution becomes lower than the conductivity of the salt solution. Since the population of vesicles increases with surfactant concentration, more K^+ and Cl^- ions are trapped inside the aqueous core thus increasing $\Delta\kappa$. The decrease in $\Delta\kappa$ at high surfactant concentrations might be due to the transformation of vesicles to rodlike micelles.

pH Dependence of Self-Assembly Structure. The fluorescence anisotropy of the DPH probe in the presence of the surfactants was also found to increase with the decrease in pH of the solution. Figure 6 shows the variations of anisotropy as a function of pH for 1 mM SAUG and SAUA. Similar changes were also observed with 5 mM surfactant solutions. The sigmoid change of the anisotropy value for both amphiphiles suggests a two-state process. This may be a result of protonation of the $-\text{COO}^-$ group that reduces ionic repulsions as well as promotes intermolecular hydrogen bonding between the $-\text{COOH}$ and $-\text{COO}^-$ or between $-\text{COOH}$ and $-\text{CONH}-$ groups at the interface as shown in Figure 4. The ordering at the aggregate interface should also result in compact packing in the interior of the bilayer aggregates as manifested by the increase of anisotropy. This means that the surface area (a_0) per surfactant headgroup is decreased. In other words, the intermolecular hydrogen bonding as a result of protonation of the $-\text{COO}^-$ group increases the curvature of the bilayer aggregates to produce closed vesicles. The inflection point of the plots in Figure 6 can be taken as the pK_a of the respective amphiphile. Thus, the pK_a values of the corresponding acid forms of SAUG and SAUA are respectively, 6.2 and 6.7. The pK_a values obtained from the inflection points

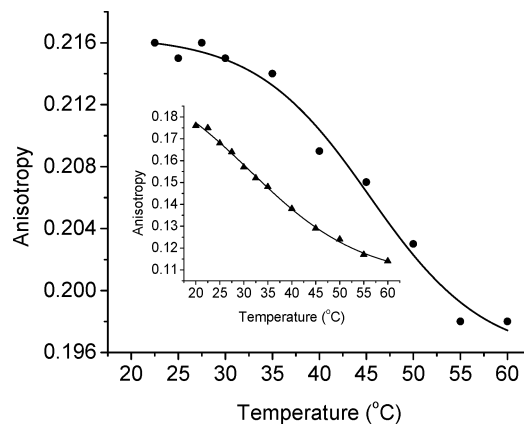


Figure 7. Plot of fluorescence anisotropy in the presence of 5 mM aqueous SAUG (pH = 8.0) against temperature; inset: plot of fluorescence anisotropy vs temperature of 5 mM aqueous SAUA (pH = 8.0).

are higher than the pK_a value of the corresponding fatty acid monomers in aqueous solution (typically 5.0).^{16a} The increase of pK_a values may be attributed to the high charge densities on the bilayer surface. A similar increase of pK_a values upon aggregation have been also suggested for fatty acids by other researchers.^{31,32} Thus, it can be concluded that vesicle structures are more favored at pH about their respective pK_a values.

Temperature Dependence of Bilayer Structure.

The phase transitions of membranes are also revealed by the fluorescence anisotropy of DPH. To determine the phase transition temperature, we have studied the temperature effect on the fluorescence anisotropy of DPH in 5.0 mM surfactant solution. The plot of the variation of r as a function of temperature is shown in Figure 7. The r value is high at low temperature, but it decreases with the rise in temperature. The large change in anisotropy at higher temperature can be associated with the phase transition between the gellike state to the liquid crystalline state. Thus, the temperature corresponding to the inflection point can be taken as the phase transition temperature, T_m . The results are included in Table 2. The high melting temperature, T_m (42 °C), clearly suggests that the vesicles are quite stable. The T_m values of the surfactants are in the order SAUA < SAUG. The higher melting temperature in the case of SAUG may be due to the stronger intermolecular amide hydrogen bonding among the surfactant molecules in the self-assembly that stabilizes the bilayer membrane structure.

Role of Intermolecular Hydrogen Bonding. The molecular structures (see Figure 4) of the amphiphiles show that there can be two stable intermolecular hydrogen bonds. The first one is between $-\text{NH}$ and $-\text{CO}$ in the amide group near the chiral center that induces a stable linear state. The second one is between the terminal amide groups of the hydrophobic chains. The influence of the amide linkage near the hydrophilic headgroup on the aggregation properties of NAAS has already been established in the literature.³³ In a recent publication, we have demonstrated the existence of intermolecular hydrogen

(31) (a) Gebicki, J. M.; Hicks, M. *Nature* **1973**, *243*, 232–234. (b) Gebicki, J. M.; Hicks, M. *Chem. Phys. Lipids* **1976**, *16*, 142–160. (c) Cisola, D. P.; Hamilton, J. A.; Jackson, D.; Small, D. M. *Biochemistry* **1988**, *27*, 1881–1888. (d) Cisola, D. P.; Small, D. M. *J. Am. Chem. Soc.* **1990**, *112*, 3214–3215. (e) Haines, T. H. *Proc. Natl. Acad. Sci. U.S.A.* **1983**, *80*, 160–164. (f) Li, W.; Haines, T. H. *Biochemistry* **1986**, *25*, 7477–7483.

(32) (a) Walde, P.; Wick, R.; Fresta, M.; Mangone, A.; Luisi, P. L. *J. Am. Chem. Soc.* **1994**, *116*, 11649–11654. (b) Bachmann, P. A.; Luisi, P. L.; Lang, J. *Nature* **1992**, *357*, 57–59.

bonding between the secondary amide groups at the end of the hydrocarbon tails of SAU.¹³ It has been shown that the intermolecular hydrogen bonding through amide bonds at the end of the hydrocarbon chain leads to the formation of bilayer structures for the SAU surfactant. The two-layer arrays of the intermolecular hydrogen-bonding interactions through the amide bonds (Figure 4) of the neighboring surfactant molecules result in the formation of a parallel arrangement of the corresponding hydrophobic tails such that the surfactant molecules can self-organize into bilayer structures in water. The secondary amide hydrogen bond chains act as a stabilizing factor to overcome hydration energies. This means that the solvation of the hydrophilic amide group near the chiral carbon will be lost during aggregation and the self-assembly will be favored by the intermolecular hydrogen bonding. The low *cac* of the amphiphiles and large size of the aggregates compared to that of corresponding fatty acid salt³² indicates that the intermolecular hydrogen-bonding interaction between amide groups enhances the hydrophobic interaction between chains, which leads to tight packing of the hydrocarbon chains. This is manifested by the low value of I_1/I_3 and high value of the fluorescence anisotropy of DPH in the self-assemblies of the amphiphiles as discussed above. The bilayer sheets with strong surface binding interactions may also tend to form spherical vesicles, ribbons, mono or multilayer tubules, and rodlike micelles. In the case of SAUA, the bilayer sheets may also get twisted due to the presence of a chiral center. In fact, homochiral interactions between the chiral groups have been proposed to account for the twisting to form the helices.³⁴ The existence of chiral aggregates, e.g., twisted ribbons and helical strands in addition to spherical vesicles and tubules, has been reported in the case of optically active NAAS by many authors.^{1–5}

Optical Activity of the Bilayer Self-Assemblies.

Formation of chiral helical aggregates is normally manifested in the CD spectra and has been demonstrated by many authors.^{5a,34–36} The aqueous solutions of SAUA were examined for chiral organization by CD spectroscopy. The CD spectra recorded in aqueous solutions of SAUA at concentrations above and below the *cac* are shown in Figure 8. The CD spectrum could not be recorded at concentrations above *cvc* because of very high absorbance of the sample. The CD spectra of SAUA in water above *cac* show a negative band at 212 nm. However, at concentrations below *cac*, the peak at 212 nm disappears and a new peak at 200 nm appears. This means that the drastic change in the CD spectrum accompanies aggregate formation. The disappearance of the CD band at 212 nm in solutions having concentrations below *cac* indicates formation of chiral structures through aggregation. The CD peak at 212 nm could be associated to the $\pi \rightarrow \pi^*$ transition of the amide bond.^{37–39} As discussed above, the amide groups of SAUA are hydrogen bonded, and therefore, their arrangement in the helical structure may be

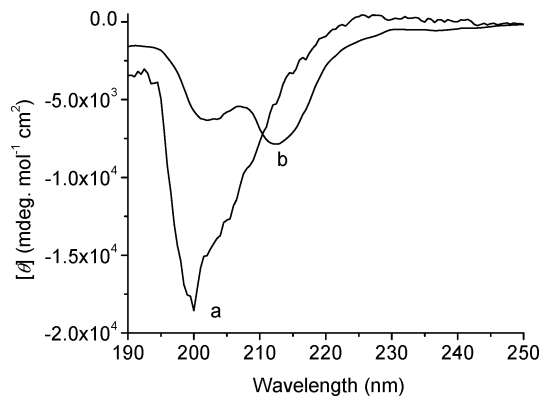


Figure 8. Circular dichroism spectra of SAUA in water (pH = 8.0): (a) 0.1 mM and (b) 2.5 mM.

similar to that in the α -helical structure of polypeptides. The CD spectra of the chiral aggregates of SAUA, however, appear to be different from those reported for amide organization in α -helix, β -sheet, or random assembly of polypeptides and proteins. The CD spectra have similarity with those of *N*-palmitoyl- or *N*-stearoyl-L-serine amphiphile in water.³⁴ This unique spectral feature as suggested by Shinitzky et al. is due to a network of the amide bonds with a distinct chiral feature.^{5a} The CD spectra seems to have originated from a repetitive arrangement of the amide bond planes on the micellar surface. Similar helical structures of chiral aggregates have also been proposed for other NAAS by various researchers.^{4b,c,37} Formation of helical aggregates of chiral amphiphiles in organic solvents has also been reported in the literature.⁴⁰

Transmission Electron Microscopy (TEM). The TEM pictures measured in 5 mM SAUG and SAUA solutions are shown in Figure 9A–C. The micrographs clearly exhibit spherical vesicles that were spontaneously formed in solution. The vesicles of SAUA have an internal diameter in the range of 60–170 nm. However, the vesicles formed by SAUG are much bigger (100–950 nm) than those of SAUA. As seen, the population of the small vesicles is large compared to the large vesicles. The absence of any recognizable structure in dilute solutions ($C < cvc$) suggests formation of flat bilayer aggregates just above the *cac*. The vesicles appear to be multilamellar type. This is evident from the micrograph in Figure 9B, which was obtained by negative staining using phosphotungstate. The micrograph clearly shows the entrapped aqueous phase and the hydrophobic lamella of the vesicle. The inner and outer diameters of the vesicle are about 300 and 445 nm, respectively. That is, the thickness of the lamella is about 145 nm. Since the hydrocarbon chain length of the surfactant is around 1.57 nm, each lamella should have thickness of about 3.14 nm. This clearly suggests that the vesicles formed by SAUG and SAUA are multilamellar.

Dynamic Light Scattering (DLS). The DLS measurements were performed to obtain the mean aggregate size of the aggregates. The average translational diffusion coefficients (D) of the aggregates were obtained from the slope of the plot (see Figure 2 in the Supporting Information) of the relaxation rates versus square of scattering vector, q^2 ($q = (4\pi n/\lambda) \sin(\theta/2)$), where n , λ , and θ are the refractive index of the solvent, wavelength of incident light and angle of scattered radiation, respectively). The plots

(33) Maeda, H.; Kakehashi, R. *Adv. Colloid Interface Sci.* **2000**, *88*, 275–293.

(34) (a) Kunitake, T.; Nakashima, N.; Shimomara, M.; Okahata, Y.; Kano, K.; Ogawa, T. *J. Am. Chem. Soc.* **1980**, *102*, 6642–6644. (b) Kunitake, T.; Nakashima, N.; Morimitsu, K. *Chem. Lett.* **1980**, 1347–1350.

(35) Sakamoto, K.; Hatano, M. *Bull. Chem. Soc. Jpn.* **1980**, *53*, 339–343.

(36) (a) Sakamoto, K.; Yoshida, R.; Hatano, M. *Chem. Lett.* **1976**, 1401–1404. (b) Sakamoto, K.; Yoshida, R.; Hatano, M.; Tachibana, T. *J. Am. Chem. Soc.* **1978**, *100*, 6898–6902.

(37) Moffitt, W. *J. Chem. Phys.* **1956**, *25*, 467–478.

(38) Gratzer, W. B.; Holtzwarth, G. M.; Doty, P. *Proc. Natl. Acad. Sci., U.S.A.* **1961**, *47*, 1785.

(39) Rosenheck, K.; Sommer, B. *J. Chem. Phys.* **1967**, *46*, 532–536.

(40) (a) Tachibana, T.; Yoshizumi, T.; Hori, K. *Bull. Chem. Soc. Jpn.* **1979**, *52*, 34–41. (b) Hidara, H.; Murata, M.; Onai, T. *J. Chem. Soc. Chem. Commun.* **1986**, 562–564.

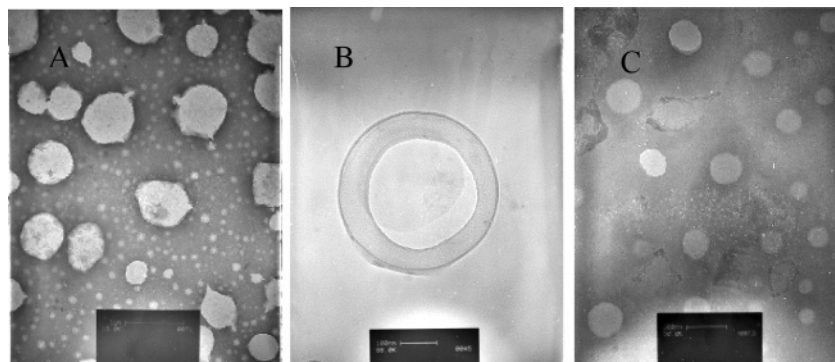


Figure 9. Negatively stained transmission electron micrographs of 5 mM aqueous solutions (pH = 8.0) of (A, B) SAUG and (C) SAUA.

are linear and pass through the origin suggesting that the apparent diffusion coefficient is due to Brownian motion of the particles. The angular dependence of the relaxation rate also suggests that the aggregates are polydispersed in size. The apparent diffusion coefficients (Table 2) of the amphiphiles are much smaller than that of normal spherical micelles ($\sim 10^{-10} \text{ m}^2 \text{ s}^{-1}$).⁴¹ Assuming spherical aggregates, the hydrodynamic radius, R_h , was calculated from the measured D value by use of Debye–Stokes–Einstein relationship. The average R_h values of the vesicles thus obtained are listed in Table 2. The results of DLS studies thus indicate the existence of large aggregates in aqueous solutions of SAUG and SAUA. The mean aggregation number (N_{agg}) of the vesicles (assuming bilayer vesicles) can be estimated by use of the equation⁴²

$$N_{\text{agg}} = 8\pi R_h^2/a_0 \quad (6)$$

The N_{agg} values thus obtained are listed in Table 2. The data indicates that the vesicles formed by SAUG and SAUA are very large. However, R_h values are smaller compared to the sizes of the vesicles shown in the TEM picture. This could be due to the fact that the solutions for DLS studies were filtered through a $0.22 \mu\text{m}$ filter. Also it should be kept in mind that DLS measures average size of the aggregates present in solution.

Conclusions

Sodium *N*-(11-acrylamidoundecanoyl)-glycinate and L-alaninate have two critical aggregation concentrations. The first, that is the lowest, corresponds to the formation of bilayer lamellar structures, and the second is due to

the transformation of a flat lamellar structure to closed spherical vesicles. The spherical vesicles, however, transform to rodlike micelles at higher surfactant concentrations ($>10 \times \text{cmc}$). The ordered bilayer membranes are spontaneously formed from the amphiphile in aqueous solution. The bilayer formation is more favored in the case of the glycine derivative. The vesicle formation is also favored in concentrated solutions and in solutions of pH at which the carboxylic group is half-protonated. The driving force for the bilayer formation is the intermolecular hydrogen bonding between the secondary amide groups of the neighboring molecules, which promote the formation of the linear array of the amphiphile molecules. As a result, the vesicles are quite stable, which is indicated by the relatively high values of phase transition temperatures of the surfactants. The microenvironment of the bilayer self-assemblies is nonpolar in nature and is highly ordered. The low translational diffusion constant and large apparent hydrodynamic radius obtained from DLS measurements suggests that the amphiphiles form large vesicles in dilute aqueous solutions. The TEM pictures of the aqueous solutions of both surfactants confirmed formation of large multilamellar vesicles. The CD spectral features suggested the presence of chiral helical aggregates in dilute aqueous solutions of SAUA.

Acknowledgment. The work presented in this paper is supported by CSIR (Grant No. 01(1664)/00/EMR-II) and DST (Grant No. SP/S1/G-36/99), Government of India. S.R. thanks CSIR for a research fellowship (9/81(380)/2002-EMR-I).

Supporting Information Available: Spectral and analytical characterization data of SAUG and SAUA, figures showing plots of conductivity as a function of surfactant concentration and decay rates versus q^2 . This material is available free of charge via the Internet at <http://pubs.acs.org>.

LA051206M

(41) Hassan, P. A.; Raghavan, S. R.; Kaler, E. W. *Langmuir* **2002**, *18*, 2543–2548.

(42) Christov, N. C.; Denkov, N. D.; Kralchevsky, P. A.; Broze, G.; Mehreteab, A. *Langmuir* **2002**, *18*, 7880–7886.